

# Characterization of Resistive Transmission Lines to 70 GHz with Ultrafast Optoelectronics

A. Deutsch, *Senior Member, IEEE*, M. R. Scheuermann, G. Arjavalingam, *Senior Member, IEEE*, L. Kneller, J. K. Tam, and C. W. Surovic

**Abstract**—The complete characterization of resistive transmission lines with the short-pulse propagation technique is extended to 70 GHz. The wide-frequency coverage is made possible by the use of ultrafast photoconductive switches for pulse generation and sampling. The picosecond optoelectronic sampling oscilloscope is described and results of measurements on thin-film strip transmission lines are presented.

RECENT advances in integrated circuit technology has resulted in the ability to fabricate high-speed microprocessors on one large silicon chip. At the same time, a computer system made-up of a few chips can be interconnected by high density thin-film wiring [1]. In both cases, transmission lines with resistive losses have to propagate signals with risetimes of 10–500 ps, over lengths of 1–5 cm. Consequently, it is important to characterize the frequency-dependent properties of these interconnections up to 100 GHz. Previously, we demonstrated a short-pulse-propagation method and signal-processing technique for determining the broadband complex propagation constant and complex impedance of a resistive transmission line, up to a frequency of 25 GHz [2]–[4]. For these results an electronic pulse generation and sampling scheme was used. In this letter, we describe the extension of the frequency coverage to 70 GHz using ultrafast photoconductive switches for pulse generation and sampling [5].

The picosecond optoelectronic sampling oscilloscope is shown schematically in Fig. 1. It consists of a pair of ultrafast optoelectronic probes capable of generating and detecting picosecond duration pulses [6]. They were fabricated on photoconductive silicon-on-sapphire substrates. For the measurements described here, a coplanar-strip design with 70  $\Omega$  characteristic impedance and a 6  $\Omega/\text{cm}$  dc resistance was used for the probes. Transmission line designs, such as coplanar waveguides, may be more appropriate for other applications. The silicon epilayer was ion-implanted to reduce its carrier lifetime to less than one picosecond [5]. The 1.5-ps wide optical pulses from a mode-locked, pulse-compressed, and frequency-doubled Nd:YLF laser were split into two beams. The 12-mW average-power pump beam was focussed between the strips of the 72 V dc-biased pulse generator probe (see Fig. 1). There it generated 200 mV amplitude electrical pulses which had an autocorrelated full-width at half maximum

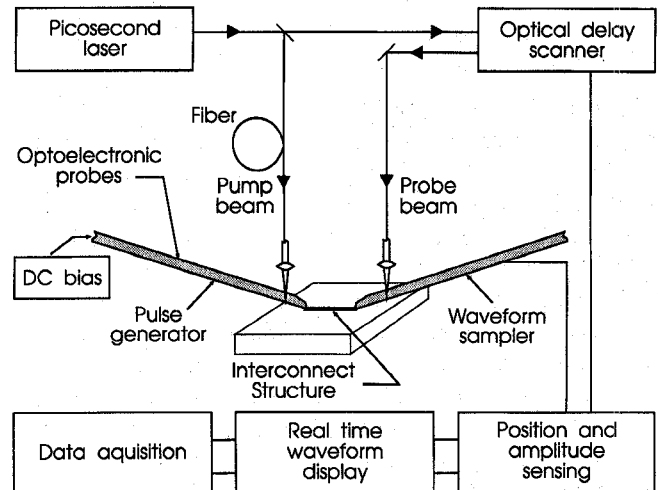


Fig. 1. Schematic diagram of the picosecond optoelectronic sampling oscilloscope.

(FWHM) of 3 ps [6]. These pulses travel to the probe tip and were launched onto the pads on the device under test (DUT) by physical contact. The pulses at the output of the DUT were coupled, also by contact, onto the waveform sampler probe where they were photoconductively sampled by the delayed probe beam [5]. A scanning delay line, which has a 300-ps span and a 0.25-ps accuracy, was used together with a computer to average, store, and display the sampled waveform [7]. The amplitude accuracy of the optoelectronic oscilloscope, which is determined by laser stability, was about 2%. An optical fiber was used to deliver the pump beam to the pulse generator. Consequently, that probe could be moved easily to any point on the sample, within a range of about 10 cm, without changing the optical delay between the two beams.

The complete characterization of resistive transmission lines by short-pulse propagation was first described in [2]–[4]. Briefly, short pulses are launched, in turn, on two different lengths of the line to be characterized. The pulse waveforms are measured at the output of the lines, digitized, and numerically Fourier transformed. Time windowing is used to eliminate unwanted reflections and retain only the forward-travelling wave. From the ratio of the complex Fourier transforms we obtain the complex propagation constant:

$$\alpha(f) + j\beta(f) = -\frac{1}{(l_1 - l_2)} \ln \frac{A_1(f)}{A_2(f)} + j \frac{\Phi_1(f) - \Phi_2(f)}{(l_1 - l_2)}, \quad (1)$$

Manuscript received October 27, 1992.

The authors are with the IBM Research Division, Thomas J. Watson Research Center, P.O. Box 218, Yorktown Heights, NY 10598.

IEEE Log Number 9207598.

where  $\alpha(f)$  and  $\beta(f)$  are the frequency dependent attenuation coefficient and propagation constant, respectively.  $A_1(f)$ ,  $A_2(f)$  and  $\Phi_1(f)$ ,  $\Phi_2(f)$  are the amplitude and phase of the Fourier transforms corresponding to lines of lengths  $l_1$  and  $l_2$ , respectively, where  $l_1 > l_2$ . It was shown in [2]–[4] that in the case of resistive lines separated by insulators with small dielectric losses ( $G \ll \omega C$ , where  $G$  is the dielectric conductance and  $C$  is the per unit length line capacitance), the complex impedance can be expressed in terms of the measured  $\alpha(f)$  and  $\beta(f)$  as

$$Z_0(f) \cong \frac{\beta(f)}{\omega C} - j \frac{\alpha(f)}{\omega C}. \quad (2)$$

It is generally found that, for low-loss insulators, the line capacitance is relatively constant over the entire frequency range of interest. Consequently, the real and imaginary parts of the characteristic impedance can be determined with the measured low-frequency line capacitance and the experimentally determined  $\alpha(f)$  and  $\beta(f)$ .

The measurement technique described above was applied to the characterization of 11- $\mu\text{m}$  wide, 3- $\mu\text{m}$  thick aluminum strip transmission lines insulated by a polyimide dielectric [1]. The wiring was fabricated with a nonplanar process typical of those used for on-chip interconnections. The structure was built on an undoped silicon substrate and consisted of top and bottom reference planes and orthogonal signal layers in-between. The lines used in this experiment were 1 and 2 cm long. They were 5.3  $\mu\text{m}$  from the bottom and 1.9  $\mu\text{m}$  from the top planes, respectively. No orthogonal wires were present. The measured lines were designed to travel in adjacent pairs having center-to-center spacings of 25  $\mu\text{m}$ . Due to the close proximity to the reference plane, mutual capacitive and inductive coupling were two orders of magnitude lower than self capacitance and inductance values, and were therefore neglected in our analysis. The measured per-unit-length dc line resistance and low-frequency (1 MHz) capacitance were 14.8  $\Omega/\text{cm}$  and 2.65 pF/cm, respectively. The polyimide dielectric constant ( $\epsilon_r = 3.25$ ) and aluminum resistivity ( $\rho = 3.56 \mu\Omega\text{cm}$ ) were determined using the measured cross sectional dimensions. Based on these values, the line capacitance  $C$  and the frequency-dependent resistance  $R(f)$  and inductance  $L(f)$  were calculated using a combination of numerical and analytical techniques [8]. For these lines, the onset of the skin effect occurs around 9 GHz and is fully developed only around 100 GHz due to the thin (3  $\mu\text{m}$ ) metallization used. This behavior emphasizes the need for accurate wide-band characterization techniques. The theoretically calculated  $\alpha(f)$ ,  $\beta(f)$  and  $Z_0(f)$  were obtained using the procedures outlined in [8].

The optoelectronically sampled waveforms at the output of 1- and 2-cm long lines were found to broaden to 14 and 32.3 ps, respectively, as shown in Fig. 2. The attenuation coefficient, phase constant and complex impedance obtained using these waveforms and the signal processing technique outlined earlier are shown as points in Fig. 3. For comparison, the theoretically calculated values are shown as dashed lines. It was found that although the lines are extremely resistive, the frequency coverage could be extended to 71.65 GHz

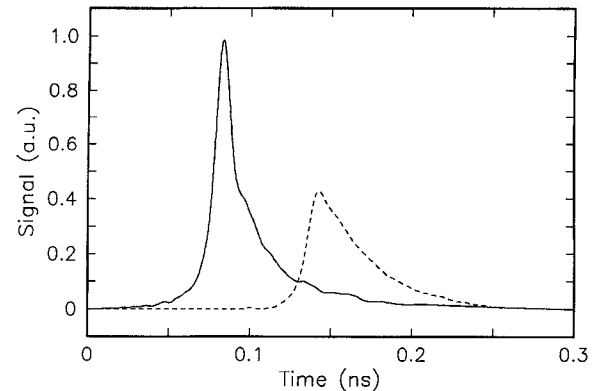


Fig. 2. Pulse waveforms at the output of 1 cm (solid trace) and 2 cm (dashed trace) long strip transmission lines with  $R_{dc} = 14.8 \Omega/\text{cm}$ .

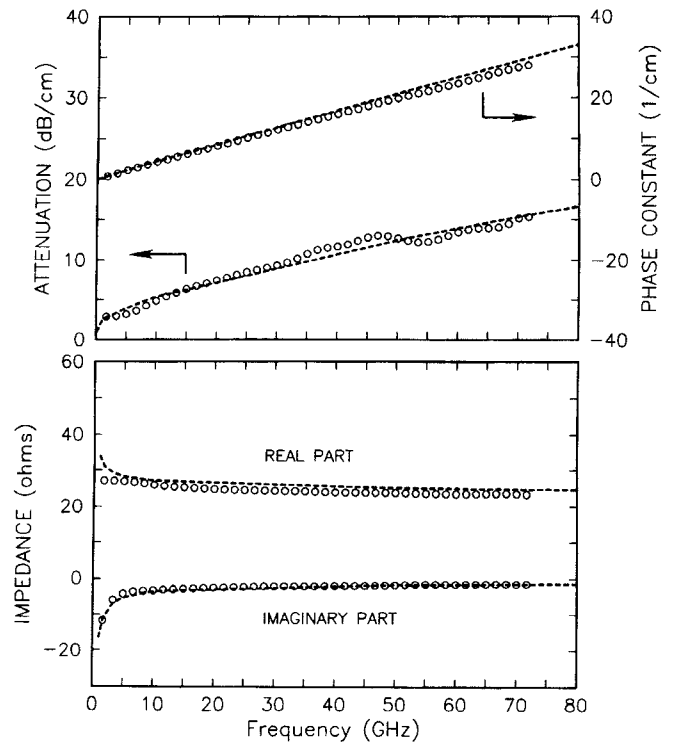


Fig. 3. Top: Attenuation coefficient  $\alpha(f)$  and phase constant  $\beta(f)$  as a function of frequency. Bottom: Real and imaginary parts of the transmission line impedance. Points are experimentally determined, dashed lines are predictions of modeling.

[2]–[4]. The worst discrepancy between calculated and measured values of  $\alpha$ ,  $\beta$ , and  $Z_0$  was on the order of 5–6 %. The calculations assumed a uniform rectangular shape for the lines, while spot cross-sectioning revealed a trapezoidal conductor shape with a  $\pm 7.5\%$  width variation along the length of a related sample.

The usefulness of the transmission-line parameters measured by the optoelectronic oscilloscope is demonstrated with the propagation of logic-like signals [2]–[4]. A 15-ps risetime step function was launched on the 2 cm long strip line and measured both in reflection (TDR) and in transmission (TDT) with a Hypres PSP-1000 oscilloscope. The measured TDR waveform is shown as a dotted line in Fig. 4. Waveforms obtained with a circuit simulation program are also shown for

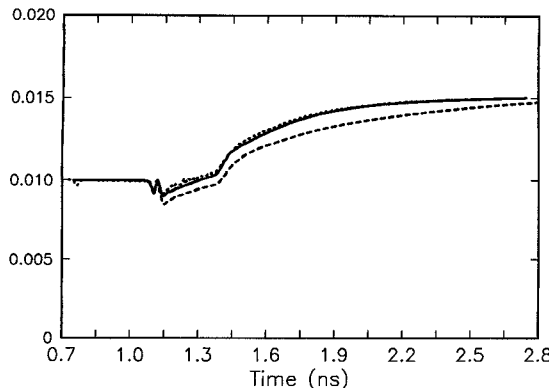


Fig. 4. TDR response of the 2-cm long thin-film line. Dotted line is measured with a Hypres PSP-1000 sampling oscilloscope. Simulated waveforms using theoretical models (dashed line) and measured properties (solid line) are also shown.

comparison [9], [10]. The dashed line used the theoretically modeled parameters, while the solid line used the characteristics determined by the short-pulse propagation technique. Clearly, the latter is much closer to the measured waveform. Similar comparisons were observed in the TDT results.

In summary, we have extended the short-pulse-propagation technique to 70 GHz using a picosecond optoelectronic sampling oscilloscope. This simple, yet powerful, procedure was used to completely characterize the frequency-dependent properties of a resistive transmission line. The use of time windowing and relative measurements on two lengths of line eliminated errors due to end effects and the need for com-

plicated calibration and de-embedding procedures. Advances in electronic circuit technology will increase the demand for higher bandwidth characterization techniques such as the one described in this letter.

## REFERENCES

- [1] M. F. Bregman, A. Kimura, T. Matsui, H. Nishida, K. Nishiyama, H. Ohkuma, and A. Tanaka, "A thin film multichip module for workstation applications," *Proc. 42nd Electron. Components & Technol. Conf., ECTC'92*, 1992, pp. 968-972.
- [2] A. Deutsch, G. Arjavalingam, and G. V. Kopcsay, "Characterization of resistive transmission lines by short-pulse propagation," *IEEE Microwave Guided Wave Lett.*, vol. 2, pp. 25-27, Jan. 1992.
- [3] D. F. Williams and R. B. Marks, "Comments on 'Characterization of resistive transmission lines by short-pulse propagation,'" *IEEE Microwave Guided Wave Lett.*, vol. 2, p. 346, Aug. 1992.
- [4] A. Deutsch, G. Arjavalingam, and G. V. Kopcsay, "Authors' reply," *IEEE Microwave Guided Wave Lett.*, vol. 2, pp. 346-347, Aug. 1992.
- [5] D. H. Auston, "Ultrafast optoelectronics," *Ultrafast Laser Pulses*, W. Kaiser, Ed. Berlin: Springer-Verlag, 1988 (and references therein).
- [6] M. Scheuermann, R. Sprik, J.-M. Halbout, P. A. Moskowitz, and M. B. Ketchen, "Ultra-high bandwidth detachable optoelectronic probes," *OSA Proc. Picosecond Electron. and Optoelectron.*, vol. 4, (OSA Proceedings Series), 1989, p. 22.
- [7] D.C. Edelstein, R.B. Romney and M. Scheuermann, "Rapid programmable 300 ps optical delay scanner and signal-averaging system for ultrafast measurements," *Rev. Sci. Instrum.*, vol. 62, no. 3, p. 579, 1991.
- [8] A. Deutsch, G.V. Kopcsay *et al.*, "High-speed signal propagation on lossy transmission lines," *IBM J. Res. Develop.*, vol. 34, pp. 601-615, July 1990.
- [9] *Advanced Statistical Analysis Program (ASTAP), Program Reference Manual*, available through IBM branch offices.
- [10] W.T. Weeks *et al.*, "Algorithms for ASTAP-A network analysis program," *IEEE Trans. Circuit Theory*, vol. CT-20, pp. 628-634, 1973.